ACTA IMEKO
ISSN: 2221-870X
September 2024, Volume 13, Number 3, 1 - 11

Analytical characterization of historical mortars from the Roman villa of Frielas (Loures, Portugal)

Tanjil Ahmmed[1,2], Ana R. Silva[3], José C. Quaresma[4], Patrícia Moita[1,2,5,6], Cristina Galacho[1,2,5,7]

[1] *ARCHMAT (Archaeological Materials Science), University of Évora, Palácio do Vimioso, Largo Marquês de Marialva, 8, 7000-809 Évora, Portugal*
[2] *HERCULES Laboratory, University of Évora, Palácio do Vimioso, Largo Marquês de Marialva, 8, 7000-809 Évora, Portugal*
[3] *Unidade de Património e Museologia, Divisão de Património Cultural e Bibliotecas, Museu Municipal de Loures, Quinta do Conventinho, km 4.3, 2660-346 Santo António dos Cavaleiros, Portugal*
[4] *CHAM - Centre for Humanities, Department of History, New University of Lisbon, Avenida de Berna, 26C. 1069-061 Lisbon, Portugal*
[5] *Associated Laboratory IN2PAST, Portugal*
[6] *Geosciences Department of School of Science and Technology, University of Évora, Rua Romão Ramalho 59, 7000-671 Évora, Portugal*
[7] *Chemistry Department of School of Sciences and Technology, University of Évora, Rua Romão Ramalho 59, 7000-671 Évora, Portugal*

ABSTRACT
The analytical characterization of mortar samples from the Roman archaeological site of Frielas, located in Lisbon, Portugal; was carried out by means of X-diffraction (XRD), thermogravimetry (TGA-DTG), optical microscopy and scanning electron microscopy coupled with energy-dispersive spectroscopy (SEM-EDS), acid attack and granulometric analysis. A total of eighteen mortar samples were collected from the different structures of the villa with different functional uses (render, filler, and floor). The results showed a similar composition of binder, while differences in aggregates allowed to establish several groups. Results were discussed as evidence of manufacturing techniques, production technologies, and provenance of possible raw materials. There was no prominent variation that can suggest a different chronology between the group of samples. Though, it is assumed that there might be some renovation, restoration, or partial rebuilding that occurred in the same period. In terms of production technology, proportions ruled by Vitruvius were not followed.

Section: RESEARCH PAPER

Keywords: mortars; Roman villa; materials; provenance; raw materials; archaeometry

Citation: T. Ahmmed, A. R. Silva, J. C. Quaresma, P. Moita, C. Galacho, Analytical characterization of historical mortars from the Roman villa of Frielas (Loures, Portugal), Acta IMEKO, vol. 13 (2024) no. 3, pp. 1-11. DOI: 10.21014/actaimeko.v13i3.1842

Section Editor: Fabio Leccese, Università Degli Studi Roma Tre, Rome, Italy

Received March 19, 2024; **In final form** September 17, 2024; **Published** September 2024

Corresponding author: Cristina Galacho, e-mail: pcg@uevora.pt

1. INTRODUCTION

The subject of this study is the analytical characterization of historical mortars from the Roman villa of Frielas, an archaeological site located in the municipality of Loures under the Lisbon district. It is on the right of the Tagus River across the Trancão river. The site has on excavation since 1997, as a result of an investigation conducted by the municipality of Loures. It was part of the territory of Olisipo (present-day Lisbon) which included a vast area ranging from Torres Vedras to the north, to the proximity of Alenquer in the east during the Roman time [1]. The territory of Loures had a strong occupation in Roman times, namely in Imperial times, with little evidence from the 2nd century AD during which there was an intense economic activity proven by the abundant import of terra sigillata. The Frielas villa fits into this chronological panorama, even revealing an extended occupation [1], [2]. Geologically, it is on the Paleogene (Eocene-Oligocene) units, over the formation identified as 'Formação de Benfica' and 'Calcário de Alfornelos' composed of conglomerates, marls, reddish sandstone, clays, and limestone [3]. Analysis of amphorae material and Terra sigillata results in continuity in the consumption patterns of this villa, from the 1st century AD to the 5th century AD; following which there appears a set of indications that point to the gradual abandonment of the villa until the beginnings of the 7th century AD (abandonment-phase). Within the wide period of effective

Figure 1. The Roman villa of Frielas; east to west orientation view (top). Peristyle wall with the embedded column, surrounded by mosaic floor and the portico (bottom).

occupation of the villa, two main construction phases had been distinguished [2], [4]: the first phase from the 1st century AD to the 3rd century AD, and the second phase from the 3rd century AD to the 5th century AD. The first construction phase has very limited structures of walls made of stone and clay. The second phase has most of the structures, with the availability of mortars. The abandonment phase has very minor structures which are mainly signs of destruction and small modifications of the second phase by using stone blocks. No traces of mortar could be found from this abandonment phase.

The architectural style of the first phase cannot be adequately recorded due to limited structural evidence. This is so because most of the structures of this phase were destroyed during the construction of the second phase. The second phase has better architectural features present. The characteristics of this second phase reflects the functionality of the spaces through the presence of some compartments that surround the peristyle with a portico and mosaic pavement passages [2]. The abandonment phase has no remarkable architectural features, except some structural remains which could have been unfinished walls or traces of destruction of earlier phases.

The urban part of the villa develops around a quadrangular peristyle, which is 17.5 m wide, with an area of about 306 m^2. It consists of two parallel walls with a water mirror in between them. These walls are made up of irregular-shaped limestone and mortar. The interior wall is 50cm wide and appears to be wider than the exterior (about 37cm) with a parietal coating composed of two layers. The central part of the peristyle appears to have been landscaped as there are no traces of pavements. The portico, about 3m wide, would have been covered by a shed, judging by the abundant presence of scattered tiles found, supported by a colonnade that would exist throughout the perimeter of the peristyle of which there are three columns bases left (embedded). The floor of the portico was covered with mosaic. On the southwest side of the Villa, some compartments were identified but their functionality is not yet clarified. The mosaic of the corridor presents a field consisting of a geometric composition delimited by a double fillet, black with inscribed squares, filled by a multiple braided and polychrome (Figure 1) [2].

For the sake of this study, a total number of eighteen mortar samples were collected from the Roman villa of Frielas. The samples were analysed by employing a multi-analytical approach to determine and characterize the components, namely binder, aggregates, and additives. As the aim of the study, the samples were chosen from the different construction areas, functionality, and structures to be compared and find out the similarities and differences. To make a correlation with the chronological sequence of the site, the results were discussed as evidence of manufacturing techniques, production technologies, and possible raw materials provenance. In the following sections starting from sample preparation, technical and instrumental conditions are discussed in the Materials and Methods section. Next, the assessment of the multi-analytical techniques is given in the Results section, and finally in the Discussion part, the results are evaluated with a comparative discussion.

2. MATERIALS AND METHODOLOGY

2.1. Sampling

All the mortar samples were collected from the 2nd construction phase of the villa, from the 3rd century AD to the 5th century AD, as the other phases have no traces or availability of mortar according to the archaeological record. The samples were collected from the different structures (water channel, peristyle, staircase mosaic floor, and mural painting wall) of the villa with different functional uses (render, filler, and mosaic floor).

2.2. Sample preparation.

Samples were prepared according to the requirements of each technique. Initially, the samples were observed for macroscopic characteristics such as colour, texture, stratigraphy, type of aggregates, and additives. When stratigraphy exists, the layers have been separated as well as the painting layers. Two different types of powders were prepared, for the thermogravimetric analysis (TGA) only global fraction (GF), and for X-ray diffraction analysis (XRD) both global and fine fraction (FF). However, the fine fraction (0.063 μm sieved fraction, rich in binder) analysis of the mortar samples was similar to the global fraction diffractograms and could not provide any additional information (Figure 2). Polished sections (cross-section) were prepared for stereo-zoom microscopy and scanning electron microscopy coupled with energy-dispersive X-ray spectrometry (SEM-EDS), and thin sections were for petrographic microscopy to identify the mineralogical composition of the mortar samples. A representative fragmented portion from each sample was used for acid attack and granulometric analysis.

2.3. Characterization methodology

The characterization methodology carried out on the mortar samples comprises a range of complementary techniques: Thermogravimetric analysis (TGA) is a thermal method in which the mass of a sample is monitored as a function of temperature or time, while the sample is subjected to a controlled temperature

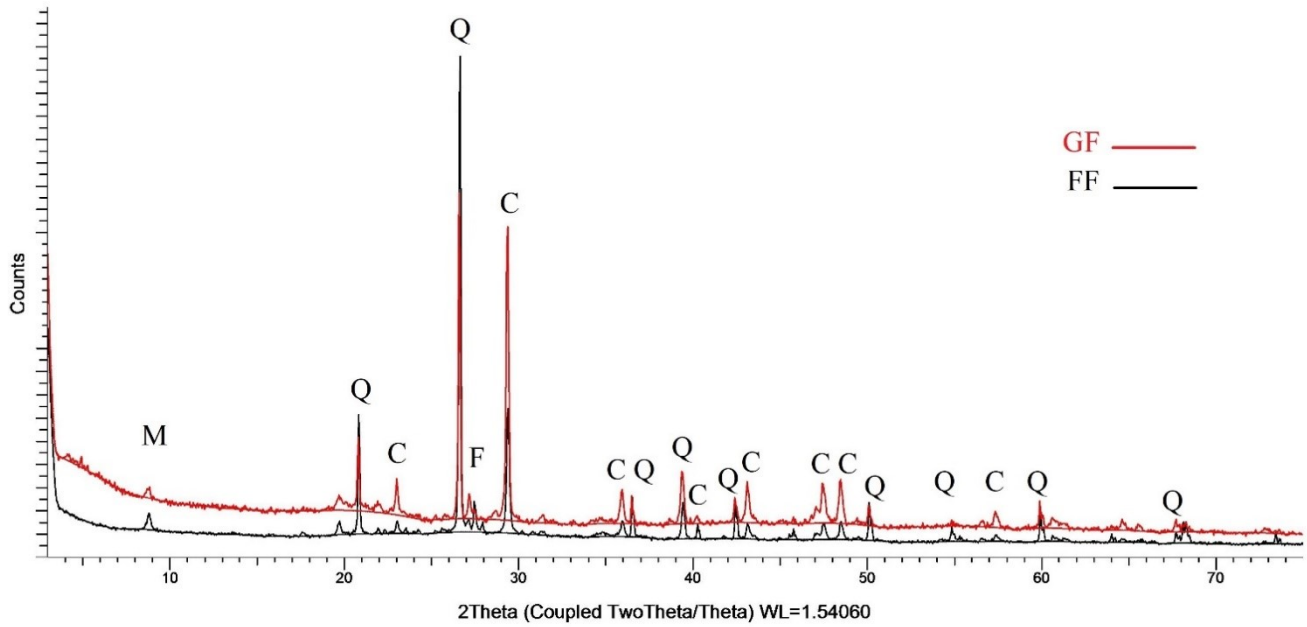

Figure 2. Global fraction (red) and fine fraction (black) shows similar result in XRD, (Q-quartz, C-calcite, F-feldspar, and M-mica).

program. For ancient mortars, the main weight loss is expected between 600°C and 900°C, confirming the decomposition of calcium carbonate ($CaCO_3$) into calcium oxide (CaO) and carbon dioxide (CO_2), which is indicative of a calcite composition of the lime-based binder [5]. Equation (1) is used to calculate the calcium carbonate content in terms of the percentage of calcite

$$CaCO_3\ (\%) = \frac{P\ (CO_2) \cdot M\ (CaCO_3)}{M\ (CO_2)}. \quad (1)$$

P (CO_2) is the percentage of mass loss between 600° and 900°C, M($CaCO_3$) is the molar mass of calcium carbonate (100.082 $gmol^{-1}$), and M (CO_2) is the molar mass of carbon dioxide (44.02 $gmol^{-1}$). The samples were analysed in a Simultaneous Thermal Analyzer STA 449-F3 Jupiter by NETZSCH, in an inert atmosphere of Nitrogen (Air Liquide Alpha-gas compressed N_2) with a flow rate of 70 mL/min. The heating program was set at a linear velocity with a constant increase rate of 10°C/min starting from 40°C and until reaching 1000°C. The quantitative analysis in the selected temperature ranges was performed by using Proteus software.

X-ray Diffraction (XRD) was used to analyse global fraction (GF) and fine fraction (FF) in order to identify the mineralogical composition and the crystalline phases of the samples. The global fraction represents the bulk sample. A Bruker D8 Discover X-ray Diffractometer was used with a Cu-Kα X-ray generator working at 40 kV voltage and current at 40 mA. The diffractograms were obtained at a 2θ, scanning between an angular range from 3° to 75° with a velocity of 0.05° per second measuring time by an LYNXEYE linear detector. The standard polymer sample holders containing approximately 1g of powdered samples were used for the analysis and the DIFFRAC. SUITE EVA software was used to identify the mineral phases with the Powder Diffraction Files of the International Centre for Diffraction Data (ICDD PDF)-2.

Scanning electron microscopy coupled with energy-dispersive spectroscopy (SEM-EDS) was used for elemental analysis, elemental mapping, and image acquisition of the mortar sample. SEM-EDS can show a higher magnification image up to x100,000 times with higher resolution and wider depth of focus, compared to optical microscopy [5]. A Hitachi S-3700N (Hitachi High Technologies, Berlin, Germany) Scanning Electron Microscope coupled with a Bruker XFlash-5010 (Bruker Corp, Billerica, Mass. USA) Silicon Drift Defector (SDD) Energy Dispersive X-ray Spectrometer was used to carry out the micro-analysis of the samples. The analysis was carried out under variable pressure, operated with an accelerating voltage of 20 kV and a chamber pressure of 40 Pa. The spectra for the chemical analysis were plotted on an energy scale of 0-20 keV with a spectral resolution of 129 eV at Mn Kα. Data were obtained in the form of elemental distribution maps, point and multipoint analysis processed with Esprit 1.9 software. The SEM images were captured in backscattered (BSE) mode, for obtaining information about the textural features of the samples.

The chemical process of attacking mortars with an aqueous solution of hydrochloric acid is used to obtain information about the ratio of the soluble fraction (carbonate binder, salts, and organic compounds) to insoluble residue (non-carbonated aggregates) present in the mortars [6].

The simplified composition of the mortars can be estimated on the basis of the method developed by Hanna Jedrzejewska for ancient lime mortars [7]. The components of mortars are considering in this method: aggregates (percentage of insoluble residue in acid attack (IR), carbonates (percentage of carbonates estimated by TGA), and acid "soluble fraction" (percentage of soluble compounds in acid, without carbon dioxide generation). The "soluble fraction" content (SF) will be expressed as a percentage and calculated using equation (2)

$$SF(\%) = 100 - IR\ (\%) + Carbonates(\%)\,. \quad (2)$$

3. RESULTS

According to the preliminary and visual inspection, the colours of the samples were mainly whitish, brownish, and reddish, though the upper layers (external) of two samples were pink (FRL-6-U) and white (FRL-19-U) in colour, respectively. The reddish samples showed a high quantity of ceramic materials

Table 1. Group of samples depending on their physical colour, aggregate types, and functions.

Group	Sample	Function	Colour	Aggregates	Physical Strength
A (Ceramic rich reddish mortar)	FRL-1	Render	Reddish	Ceramics, coarse sand	Strong
	FRL-3	Render	Reddish	Ceramics	Strong
	FRL-5	Render	Reddish	Ceramics	Strong
	FRL-7-i	Floor	Reddish	Ceramics and sand	Strong
	FRL-9	Floor	Reddish	Ceramics	Strong
	FRL-10D	Filler	Reddish	Ceramics	Strong
B (Quartz rich whitish mortar)	FRL-2	Render	Whitish	Ceramics, coarse sand	Strong
	FRL-4	Filler	Whitish	White sand	Mild strong
	FRL-6D	Render	Whitish	Fine ceramics and sand.	Mild strong
	FRL-7-ii	Floor	Whitish	White sand	Mild strong
	FRL-8D	Floor	Whitish	White sand	Mild strong
	FRL-12	Filler	Whitish	White sand	Mild strong
C (Shell & basaltic brown mortar)	FRL-11-i	Render	Brownish	Brown sand	Fragile
	FRL-11-ii	Render	Brownish	Brown sand	Fragile
	FRL-15	Render	Brownish	Brown sand and shell	Fragile
	FRL-17	Render	Brownish	Brown sand and shell	Fragile
	FRL-18	Render	Brownish	Brown sand	Fragile
	FRL-19D	Render	Brownish	Brown sand	Mild strong
D (Binder rich upper layers)	FRL-6U	Render	Pinkish	Fine ceramics and sand.	Mild strong
	FRL-8U	Floor	Whitish	White sand	Mild strong
	FRL-10U	Filler	Yellowish	Ceramics	Mild strong
	FRL-19U	Render	Whitish	White sand	Mild strong

(fragments and powder). The whitish samples were mainly filler and render mortars. The samples FRL-17 and FRL-18 had chromatic layers with dark brown and brown thin pigmented layers, respectively. FRL-19 was collected from the wall of a compartment that appears to have been decorated with plasterwork. For all the samples with stratigraphic layers, it was observed that the upper layers were binder rich with smaller siliceous aggregates than the lower layers. Sample FRL-8 contains tesserae (Black, red, and white) in a whitish binder matrix as the upper layer (FRL-8-U). It was observed that some of the samples have visible cracks (FRL-1, FRL-3) and lime lumps (FRL-4, FRL-10, FRL-12). Shells or fragments of shells (FRL-15, FRL-17) and basalt (FRL-1, FRL-18, FRL-19) as aggregates were also detected. Crushed ceramics fragments show up as large-sized (20-30mm; FRL-1, FRL-7-i, FRL-9, FRL-10) and medium-sized (10-20mm; FRL-3 and FRL-5).

Following this observation, the samples were mainly divided based on their physical colour. Group A, ceramic rich reddish mortar (opus signinum). Group B quartz and brownish mortar (render) as group C that contains shell & basalts. Upper layers (external) of all stratified samples are in the group D. The resistance of the samples was also observed during the experiment of the disaggregation process using a rubber hammer and chisel, wherein it was noticed that all the samples with crushed ceramics or ceramic fragments as aggregates were stronger in terms of physical strength. The whitish samples which contain siliceous aggregates in the binder-rich matrix were mostly with medium physical strength and in some cases fragile as well (FRL-4, FRL-12). The samples in brownish colour (including samples with paint) were mainly weak in strength and fragile (FRL-15, FRL-17, FRL-18) (Table 1).

This group separation, based on the type of aggregates, was corroborated by the different techniques applied. Petrographic analyses (Figure 3) show the predominance of ceramic fragments, with minor quartz, feldspar, and mica where they show sub-angular shapes on group A.

On the other hand, group B shows higher quantity of quartz and feldspars grains (K-feldspar and plagioclase) in angular and sub-angular form. Although quartz grains have been mainly observed as single grains, in a few cases it was present as part of lithic fragments such as quartzite or associated with feldspars as granitic grains. Group C have quartz and feldspar along with the basaltic grains which were mostly rounded and sub-angular shaped. In some cases, alteration of olivine with the presence of iron-oxide can be seen in association with basaltic grain or glassy textural grain while this group also contain seashells. As previously described, external layer of the samples is in the Group D, which has quartz and carbonated grains (FRL-19) as aggregates. By means of the Optical Microscopy (OM), stereo zoom microscopy observation and insoluble residue from the

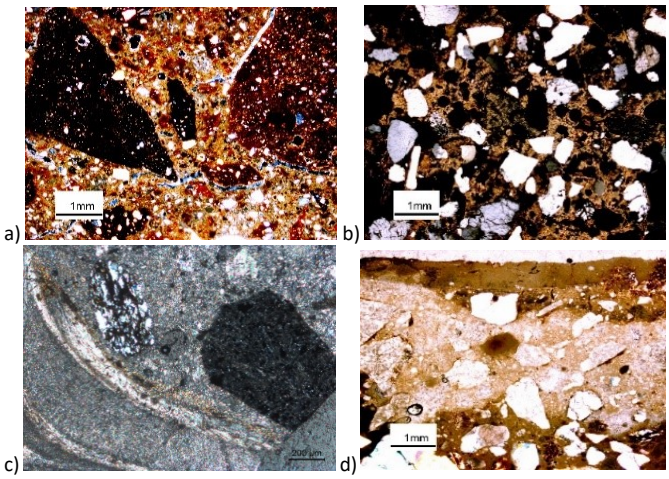

Figure 3. a) Angular shaped ceramic fragments with fine cracks. Finer ceramic dust in lime binder (FRL-3, Group-A). b) Aggregates distribution in lime rich binder. Predominance of quartz and feldspar (FRL-12, Group-B). C) Shell fragments, rounded shape basaltic grain (FRL-17, Group-C). d) Lime rich paint (top), lime rich binder with limestone and crushed lime fragments (FRL-19U, Group-D).

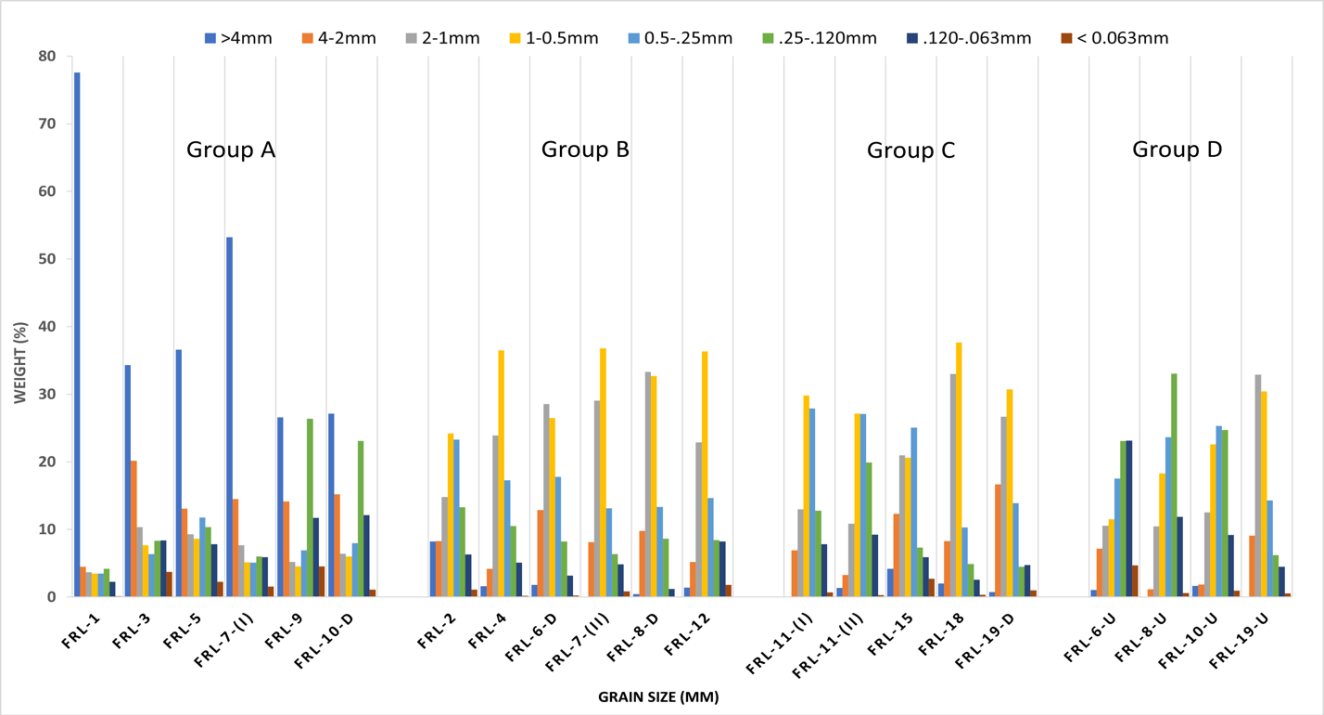

Figure 4. Grain size distribution of all the group of samples.

acid attack analysis, the grain size and shape of the aggregates were observed mainly angular to sub-angular.

The granulometric analysis of the previously grouped samples shows patterns (Figure 4) of particle size among the samples as grain size distribution plotted in grain chart. Sample with the ceramic as group-A has an abundance in grain size of greater than 4mm (weight %), while the rest of the sample (Group-B and C) shows similarity with an abundance in grain size of 1-0.5mm (weight %).

SEM-EDS helped for the characterization of aggregates and binder; the EDS elemental map shows the presence of quartz with silicon, while feldspar has been detected with the presence of aluminium and silicon, in association with either potassium or sodium that are present in all the groups (Figure 5). In Group A, ceramic fragments were detected by their siliceous inclusions

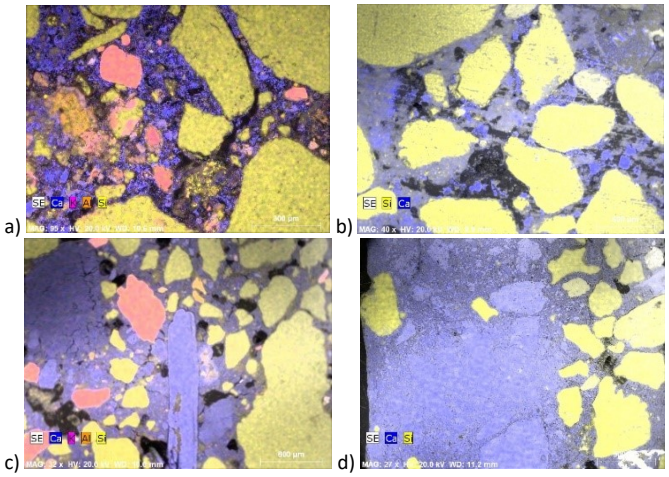

Figure 5. a) FRL-10, Group-A. b) FRL-8, Group-B). C) FRL-15, Group-C). d) FRL-19U, Group-D). The aggregates are mainly Si rich sub-angular to angular shape quartz and Feldspar. The upper layer of the samples has more Ca rich binder and Carbonated aggregates.

(e.g., quartz and feldspars) in an aluminium-potassium matrix according to phyllosilicates composition. Additionally, cracks developed alongside the ceramic fragments and sometimes within the binder matrix. Though, there is no significant zoning, boundary marks, or pozzolanic reaction observed in SEM-EDS images. Samples with shell fragments belongs to group C mortars. Samples containing basaltic rock fragments appear with minerals that might be associated with olivine and pyroxene.

The presence of Mg, Fe, Si, Ca, and Al is indicative of mafic minerals and plagioclase, respectively (Figure 6a). The rounded shape of this kind of aggregates is almost similar in the group C mortars. The morphological characteristics indicate their significant transportation from their geological source of origin.

Area analysis were carried out to identify the lime lump composition of the samples; the result demonstrates that the lime lump is mainly composed of Ca, C and O that is a limestone should be used as raw material to produce calcite areal lime (Figure 6c and d). Area analysis revealed that the binder composition was similar to all samples which is mainly composed of Ca as an indicative of lime binder. A high amount of Ca in the binder composition with a very low percentage of Mg was noted. The presence of other elements such as K, Al, and Si, and Na may be influenced by aggregates.

X-ray diffraction (XRD) results confirm the mineralogical composition of K-feldspar (orthoclase and microcline) in all of the mortar samples (Table 2). In Group A, we found traces of micas (muscovite or biotite) within the samples (Figure 7), while into the group B there were no traces of micas and a predominance of quartz, feldspar, and calcite. Group C can be differentiated by the presence of pyroxene, and hematite which could be associated with basaltic lithic fragments. Group-D has abundance of calcite and quartz.

In TGA, the percentage of calcium carbonate as a function of the mass losses in the temperature range between 600°-900°C, recorded from the thermogram, showed that the calculated $CaCO_3$ amount ranges from 12.7% (FRL-5, Group-A) to 64.6%

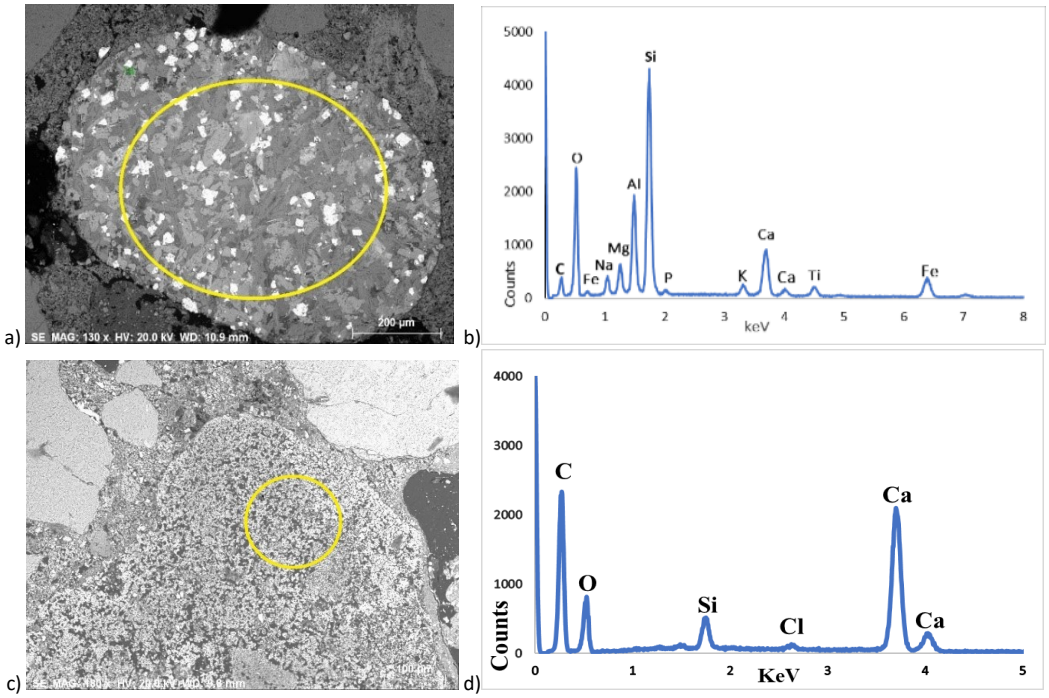

Figure 6. a) rounded basaltic grain in BSE image (FRL-19, Group-C), b) multi-point analysis spectrum from image 'a'. c) yellow line indicating lime lump (FRL-17, Group-C), d) multi-point analysis spectrum of the spot marked in image 'a'.

Table 2. Mineralogical composition of the global fractions of mortars assessed by XRD.

	Sample	Quartz	Calcite	K-Feldspar	Plagioclase	Pyroxene	Hematite	Micas
A (Ceramic rich reddish mortar)	FRL-1	+++	++	+	T	T	T	+
	FRL-3	+++	+	++	T	-	-	+
	FRL-5	++	+	++	+	-	-	+
	FRL-7-i	+++	+	++	++	-	T	+
	FRL-9	++	+	++	T	-	-	+
	FRL-10-D	+++	++	++	+	+	T	+
B (Quartz rich whitish mortar)	FRL-2	++++	+	++	T	-	-	-
	FRL-4	+++	++	++	+	-	-	T
	FRL-6-D	++++	+	++	T	-	-	T
	FRL-7-ii	++++	+	++	T	-	-	T
	FRL-8-D	++++	+	++	T	-	-	-
	FRL-12	++++	+	++	-		-	T
C (Shell and basaltic brown mortar)	FRL-11-i	+++	+	++	-	T	-	-
	FRL-11-ii	++++	+	++	T	T	-	T
	FRL-15	++	+	+++	-	T	T	T
	FRL-17	++	+	++	T	T	-	T
	FRL-18	+++	+	++	-	T	-	T
	FRL-19-D	++	+	++	T	T	-	T
D (Binder rich upper layers)	FRL-6-U	++	+	+++	T	-	-	T
	FRL-8-U	++	+++	++	T	-	-	-
	FRL-10- U	+++	+	++	T	-	-	T
	FRL-19-U	++	+++	+	T	-	-	-

++++ Predominant, +++ abundant, ++ major, + minor, T- trace

(FRL-19-U, Group-D) (Figure 8) among the samples. The average of the soluble fraction ranges from 18.35% (FRL-1) to 76.60% (FRL-19-U) whereas the insoluble residues vary between 23.30% (FRL-19-U) to 81.35% (FRL-1) (Table 3).

4. DISCUSSION

Based on the results obtained from OM, XRD, TGA, and SEM-EDS, mortar samples from the Roman villa of Frielas presents in general a calcitic lime binder; the significant detection of calcite by XRD associated with the TGA thermogram, showing greater mass losses in the characteristic range between temperature 600°C - 900°C as well as the presence of Ca on elemental maps of EDS points to a binder with calcitic composition. Moreover, the acid attack analysis allows the determination of the soluble fraction. Though, the partially dissolved carbonate aggregates (e.g., shell fragments) might overestimate the amount of calcium carbonate present in the

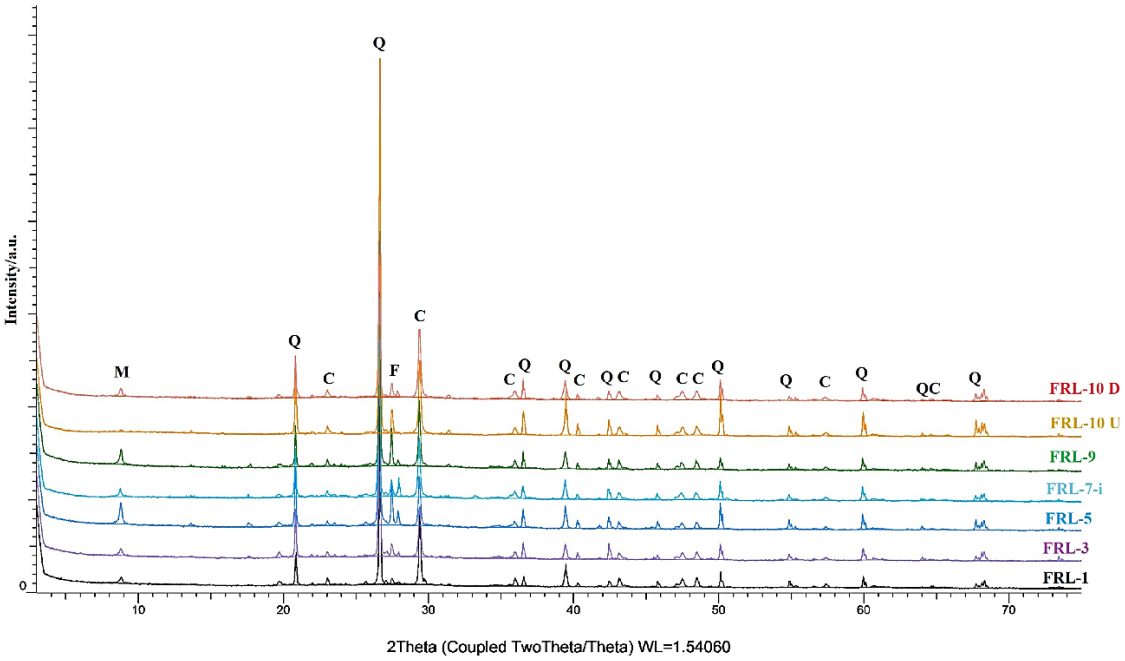

Figure 7. XRD patterns (Global fraction) of ceramic rich samples (Group-A), (Q-quartz, C-calcite, F-feldspar, and M-mica).

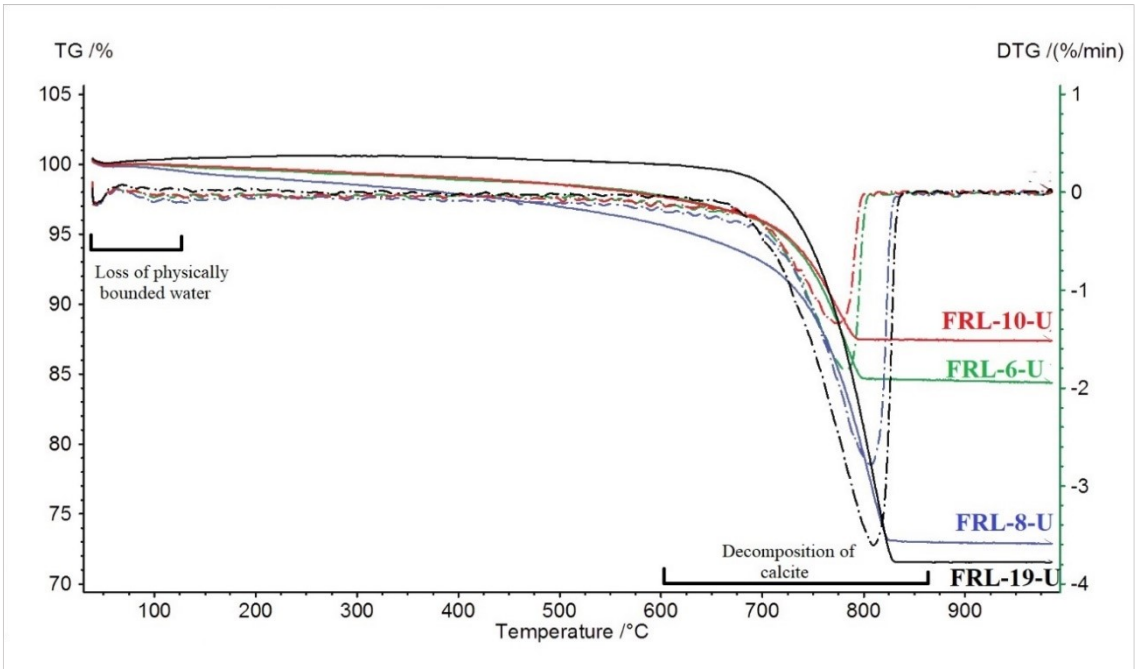

Figure 8. TG/DTG curves of binder-rich upper layers (Group-D) samples FRL-6-U (green), FRL-8-U (blue), FRL-10-U (red), and FRL-19-U (black), continuous curves representing TG and dashed curve representing DTG data.

samples. The amount of calcium carbonates from acid attack (soluble fraction), XRD, and TGA can be compared (Figure 9).

The lime lumps present in a few samples provide information about raw materials used for calcination during the binder preparation. The analysis on the lime lumps of the studied samples indicates the presence of Ca, O, and C, which represents calcium carbonate ($CaCO_3$) thereby indicating a calcitic areal binder.

In group A, the samples containing crushed ceramic fragments correspond to the water channel structure as their functions are associated with a waterproofing mortar and opus signinum [8]. The size of the big, crushed ceramic in sample FRL-1 (water channel-surface) was similar to other opus signinum samples (FRL-9, and FRL-7-i). In that case, as opus signinum, FRL-9 contains big, crushed ceramics (2-3 cm) such as FRL-1 and FRL-7-i. While FRL-10-D being in the same group and same construction phase (2nd phase), contains smaller (0.25-0.125 mm to 4-2 mm) ceramic fragments than others which might indicates different preparation.

During the sample collection, we wanted to compare the inner sides of the parallel water channel. The inner side of the two walls are coated with opus signinum, functioning as a waterproofing element FRL-3 and FRL-5 (group A) that contains ceramic fragments (> 4 mm). The results indicate that

Table 3.Simplified composition of the mortars.

Group	Sample	Soluble fraction (%) [1]	Insoluble residue (%) [2]	$CaCO_3$ (%) [3]	Binder: Aggregates Ratio
A (Ceramic rich reddish mortar)	FRL-1	-2.4*	81.3	21.1	1:4
	FRL-3	8.1	77.1	14.8	1:6
	FRL-5	8.7	78.6	12.7	1:7
	FRL-9	12.6	70.8	16.5	1:5
	FRL-7 i	4.5	77.8	17.7	1:5
	FRL-10-D	10.1	66.1	23.8	1:3
B (Quartz rich whitish mortar)	FRL-2	10.6	65.4	24.0	1:3
	FRL-4	8.4	60.5	31.1	1:2
	FRL-6-D	2.8	77.3	19.8	1:4
	FRL-7 ii	3.6	73.6	22.7	1:3
	FRL-8-D	4.9	81.1	13.9	1:6
	FRL-12	10.1	67.7	22.2	1:3
C (Shell & basaltic brown mortar)	FRL-11 i	5.7	68.2	26.1	1:3
	FRL-11 ii	6.1	66.4	27.5	1:3
	FRL-15	0.6	70.4	29.0	1:2
	FRL-17	-	-	29.0	1:2**
	FRL-18	0.45	70.9	28.6	1:3
	FRL-19-D	7.2	70.5	22.3	1:3
D (Binder rich upper layers)	FRL-6-U	11.8	57.8	30.3	1:2
	FRL-8-U	15.5	32.5	51.9	1:1
	FRL-10-U	8.6	68.1	23.3	1:3
	FRl-19-U	12.1	23.3	64.6	2:1

1. Soluble = 100- ∑(insoluble residue + carbonates).
2. Insoluble residue percentage from Acid attack analysis.
3. Calculated wt. % of $CaCO_3$ (from TGA analysis)

* The calculated negative value can be due to the heterogeneity of the samples obtained from both analyses (acid attack and TGA).

** In the case of Sample FRL-17, was calculated only depending on the carbonates % obtained from TGA, due to unavailability of enough sample for an acid attack.

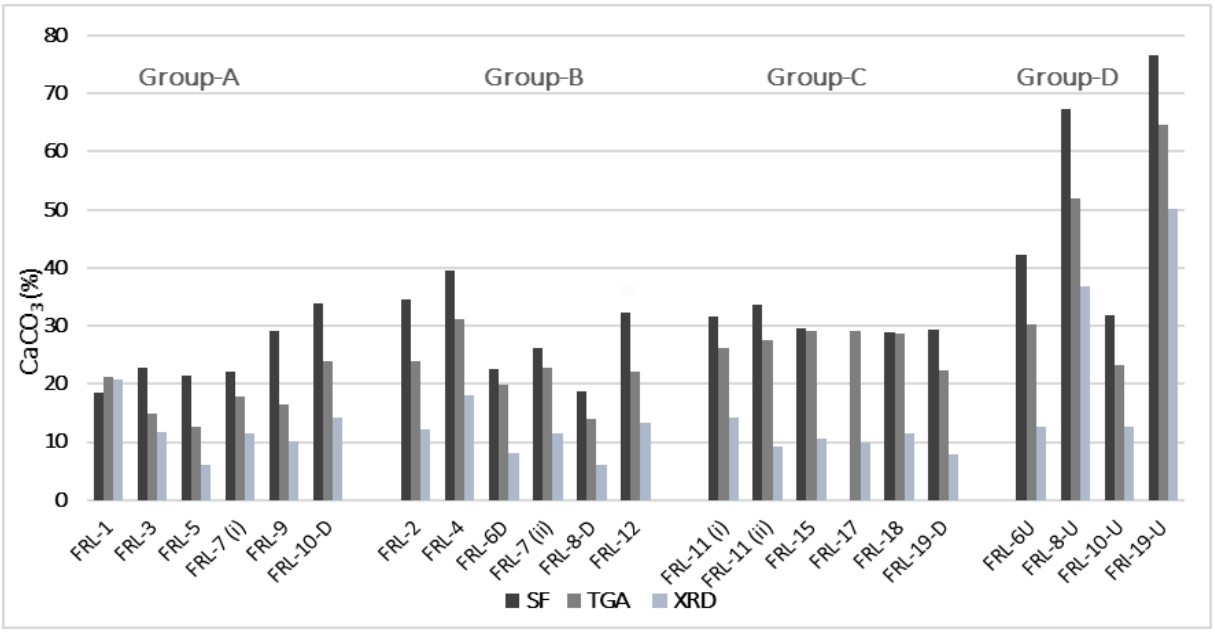

Figure 9. Amount of $CaCO_3$ (weight %) of the studied samples. Comparison of TGA, acid attack (Soluble fraction), and XRD. XRD is giving semi-quantitative analysis from GF (Global fraction).

the samples FRL-3 and FRL-5 show similar characteristics, while a layer FRL-2 (group B) adjacent to the FRL-3 shows different features, since it has a rough or uneven texture, and seems prepared for receiving a final layer, perhaps stucco. Sample FRL-2, have a predominance of siliceous minerals aggregates, associated with very few and smaller random crushed ceramic fragments. These features suggest a different preparation of mortars associated with a circumscribed later renovation.

According to several authors, the roman mosaic floor composition has several mortar layers (Figure 10a). The second layer as 'bedding' is a thin layer which is rich in lime. Usually, in this layer the mosaic design is being marked and the tesserae design usually inserted before the mortar get hardened. The third layer 'Nucleus' is an impermeable mortar layer of powdered pottery and lime, to protect the mosaic from the soil water (humidity) [9], [10]. As the mosaic floor sample, FRL-8 (group B) shows differences, mainly in the layering and absences of ceramic in 'Nucleus' layer (Figure 10b and c). Though, samples from group A, has the association to the floor (FRL-7i), and compartment floor (FRL-9) as opus signinum which contains

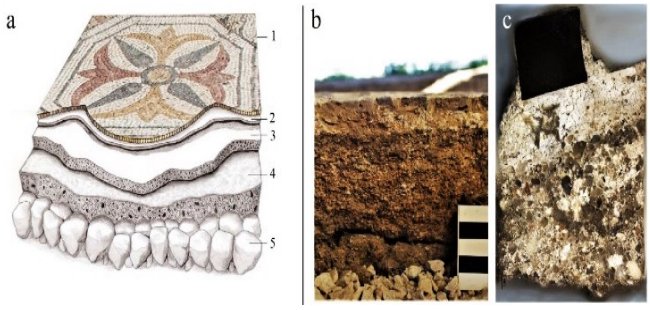

Figure 10. a) Stratigraphy of a Roman mosaic floor according to Vitruvius's description. ('a' Adapted from Caldeira et. al., 2019). 1. Tessellatum, 2. Bedding, 3. Nucleus, 4. Rudus, 5. Statumen, b) section view of the sample FRL-8 (mosaic floor) in situ, from the site, c) prepared polished section of the sample FRL-8, containing stratigraphic layers of the floor.

crushed ceramic thus indicate FRL-8 being in the same construction phase (2nd phase) followed different preparation.

The third group (group C) demonstrates a different aggregates assembly within the samples. The samples of this group are from structural detachments (mural painting), and from the wall of the compartments. The predominance of siliceous aggregates in this group is as similar as other groups with the presence of quartz and feldspar, but containing calcitic shells and rounded basaltic grains distinguish the group from others. The rounded shape of these basaltic rock fragments indicates a particular transportation from the geological origin and different sources of aggregates from the other groups.

For the determination of the provenance study of the samples, the lime used in the mortars of the Roman villa of Frielas is calcitic in nature, thus corresponding to an aerial lime. The degree of purity of the lime, without a significant siliceous (detrital) contribution, suggests limestones as the raw material been used. This lithology according to available cartography is abundant in the surrounding geological context. Namely represented by limestones of formations from 'Calcário de Alfornelos' and 'Formação de Bica calcário' [11], [12]. Also, in addition to the limestone formations, the villa is based on the Benfica formation which is according to present limestones intercalations (formation of arranó). Thus, within a distance radius of 5 km, it is possible to obtain the limestone compatible with the lime composition.

The morphology of the aggregates of the samples are mainly angular to sub-angular or even poorly rounded that might indicate a short distances transportation from the source of origin but in a different geological context and surroundings of the *villa*. On the right bank of the Tagus River, sand is available in the lower Miocene units between Lumiar, Ameixoeira, Aeroporto, Charneca, and Camarate. Therefore, it can be assumed that the possible sources of sand (quartz and feldspar) were more accessible from the right bank of the Tagus River.

Sample with shell and basalts were previously described as group C. The basaltic rock fragments are observed as rounded shapes. This detail indicates transportation from their geological source, most probably the 'Complexo Vulcânico de Lisboa' (CVL), contributing to some region's alluvial sediments-together with shells.

The sample with crushed ceramics corresponding to the hydraulic structure and opus signinum. Their size and shape differ from the functionality of the mortar. These ceramic fragments are assumed as brick and tiles fragments.

The method of Jedrzejewska [7] was used to determine the binder to aggregate ratios, revealing the production technology of mortar. The ratios obtained from the result shows very random pattern that does not fit into the previously discussed groups. However, the ratios are found in two different patterns, 1st pattern of samples ratio is 1:3, and 2nd pattern of samples ratio is 1:1 to 1:7. No certain conclusions can be made based on the assessment employed for the binder aggregate ratios.

Vitruvius in his work suggested different binder to aggregate proportions depending on the types of sand, in the case of pit sand, three parts of sand should be combined with one part of lime (1:3); in the case of river or sea-sand, two parts of sand and one part of lime (1:2); and for a "better composition," the third part of sieved powdered brick might be used (Book II, Chapter V, Vitruvius). According to Vitruvius's description, 1:3 can be an 'ideal proportion' in the case of pit sand, the studied samples are resulting in the analysis that can comply with the river sand. The binder to aggregate ratio 1:3 can be considered as a pattern of contemporary structural mortar which might be prepared following roman recipe, while the rest of the samples, with other proportions, can be an indication of repair, rebuild (extension), or renovation of the structures.

The inaccuracy of the proportions of aggregates added to the mixture can also be due to the inaccessibility to traditional recipes and a construction based on empiric and intuitive knowledge and a "trial and error" practice or the result of an inexperienced labourer. The remoteness of this rural environment might have influenced the lack of qualified masons, who were most likely to live in the bigger cities [13].

Samples were also studied in terms of their level of hydraulicity. The hydraulicity of the mortars was calculated based on the results obtained by TGA analysis, the ratio between carbon dioxide (CO_2) to structurally bounded water (H_2O) in relation to carbon dioxide (CO_2) to make a correlation with the hydraulic degree of the mortars (Table 4). The hydraulicity of different types of mortars has been studied and it was determined that the "inverse trend of hydraulicity of mortars is being augmented exponentially with CO_2" [14], in which the lower the

Table 4. Weight loss percentages of structurally bound water in the temperature range 200-600 °C, and CO_2 (600-900 °C) for understanding the hydraulic characteristic of the samples.

Group	Sample	H_2O (%)	CO_2 (%)	CO_2/H_2O
A	FRL-1	2.96	9.31	3.1
	FRL-3	3.20	6.55	2.0
	FRL-5	2.08	5.60	2.7
	FRL-7-i	2.43	7.79	3.2
	FRL-9	3.18	7.30	2.2
	FRL-10-D	2.62	10.47	4.0
B	FRL-2	2.02	10.60	5.4
	FRL-4	1.81	13.72	7.5
	FRL-7-ii	0.89	10.00	11.2
	FRL-6-D	1.17	8.72	7.4
	FRL-8-D	1.25	6.12	4.8
	FRL-12	1.42	9.77	6.9
C	FRL-11-i	2.15	11.52	5.3
	FRL-11-ii	1.68	12.11	7.2
	FRL-15	0.63	12.79	20.3
	FRL-17	1.24	12.76	10.2
	FRL-18	0.71	12.60	17.5
	FRL-19-D	1.21	9.81	8.1
D	FRL-6-U	1.79	13.27	7.4
	FRL-8-U	3.38	22.70	6.7
	FRL-10-U	2.04	10.26	5.0
	FRL-19-U	0.57	28.42	49.8

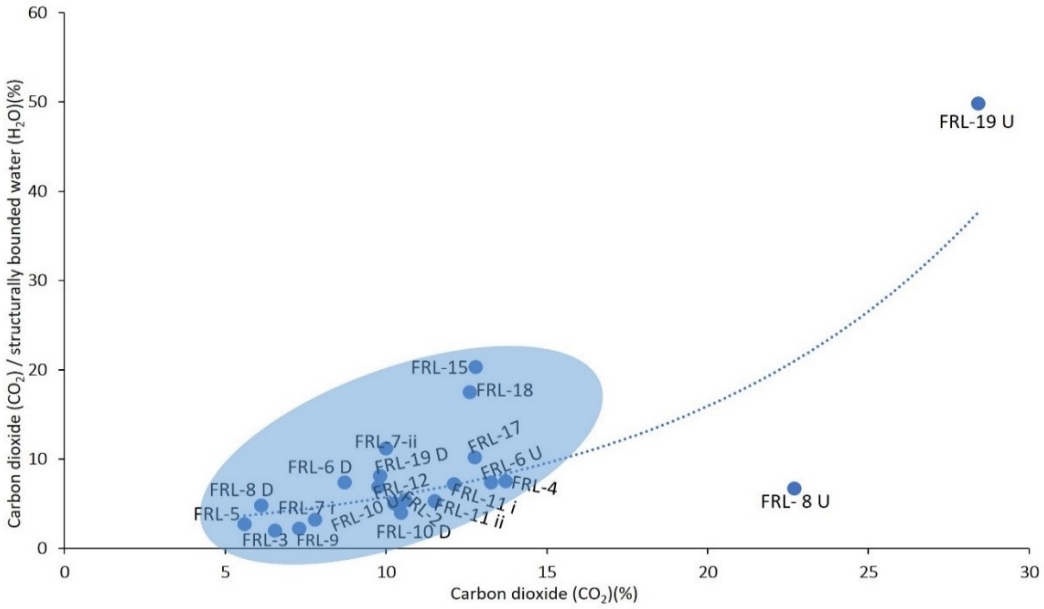

Figure 11. The chart indicating assemblage of the samples with hydraulic characteristics depending on the CO_2/H_2O in relation to CO_2.

ratio is, the higher the hydraulicity. If the ratio of CO_2/H_2O is between 1 and 10, mortars can be accepted as hydraulic [14], [15], [16].

Results indicate that most of the samples plotted (Table 4) is in the same assemblage (Figure 11) depending on the relationship between CO_2 to structurally bonded water ratio versus CO_2 mass loses according to their hydraulic characteristic. Most of the samples including ceramic-rich samples have hydraulic characteristics depending on the CO_2/H_2O in relation to CO_2.

Though sample FRL-19-U and FRL-8-U show different positions in the chart, due to their high amount CO_2 (%) and low H_2O percentages which is because of their binder-rich properties that comply with their functionality.

5. CONCLUSION

The study aimed to understand the composition and chronological sequence of mortars from the Roman villa of Frielas. By characterizing the materials in terms of binder and aggregates, evidence was provided for the raw materials used and their local provenance. The production techniques were compared to ancient recipes from Vitruvius. Samples were categorized based on aggregate differentiation, revealing a uniform composition of mortars with a calcitic areal binder and siliceous aggregates such as quartz and feldspar. Some samples also contained ceramic, shell, or basaltic rock fragments, likely sourced locally from the geological formations nearby. The binder-to-aggregate ratio varied among samples, challenging the ideal proportions suggested by Vitruvius. Despite this, the mortars exhibited hydraulic characteristics. Overall, the mortars showed uniformity in chemical, mineralogical, and microstructural composition, suggesting contemporaneous manufacturing. The study suggests that while Vitruvius' rules were not strictly followed, masons likely relied on their expertise and available materials for construction purposes. This research provides valuable insights into ancient construction practices and may inform future efforts in structural conservation and restoration of the site.

ACKNOWLEDGMENT

The authors wish to acknowledge "Laboratório HERCULES - Herança Cultural, Estudos e Salvaguarda" funded by FCT – Fundação para Ciência e a Tecnologia, I. P. under reference UIDB/04449/2020, (DOI: 10.54499/UIDB/04449/2020) and "IN2PAST – Associate Laboratory for Research and Innovation in Heritage, Arts, Sustainability and Territory" funded by FCT – Fundação para Ciência e a Tecnologia, I. P. under reference LA/P/0132/2020 (DOI 10.54499/LA/P/0132/2020).

REFERENCES

[1] R. Silva, A villa Romana de Frielas – espaço, tempo e funcionalidade, Arqueologia como Documento, Catálogo de Exposição, Câmara Municipal de Loures, 2004. [in Portuguese]

[2] A. R. Silva, Villa Romana de Frielas, Cira-Arqueologia, vol.1, 2012, pp. 88-102. [in Portuguese]

[3] T. M. Azevêdo, A. M. G. Carvalho, M. S. Oliveira, C. Romariz, O "Complexo de Benfica" na Região de Lisboa, Estudo Sedimentológico. Comunicação do Serviço Geológico de Portugal, Lisboa, vol.77,1991, pp. 103-120. [in Portuguese]

[4] J. C. Quaresma, A villa de Frielas na Antiguidade Tardia: evolução estratigráfica entre c. 410 e 525-550 d.C, Mediaeval Sophia, vol.19, 2017, pp.425-448. [in Portuguese]

[5] B. H. Stuart, Analytical Techniques in Materials Conservation, John Wiley & Sons Ltd., England. ISBN: 0-470-01280-3. 2007, pp.72-108.

[6] B. Middendorf, J. J. Hughes, K. Callebaut, G. Baronio, I. Papayianni, Investigative methods for the characterization of historic mortars- Part 2: Chemical characterization, Materials and Structures, v-38, 2005, pp. 771-780. DOI: 10.1007/BF02479290

[7] H. Jedrzejewska, Old Mortars in Poland: A New Method of Investigation, Studies in Conservation, vol.5, 1960, pp. 132–38. DOI: 10.1179/SIC.1960.021

[8] A. R. Silva, A estação arqueológica de Frielas, In Actas do 30 Congresso de Arqueologia Peninsular. VI. Arqueologia da Antiguidade na Península Ibérica. Porto: ADECAP, 2000, pp. 481-489. [in Portuguese]

[9] B. Caldeira, R. J. Oliveira, T. Teixidó, J. F. Borges, R. Henriques, A. Carneiro, J.A. Peña, Studying the Construction of Floor Mosaics in the Roman Villa of Pisões (Portugal) Using

Noninvasive Methods: High-Resolution 3D GPR and Photogrammetry, Remote Sensing, vol.11 (16), 2019, 1882. DOI: 10.3390/rs11161882

[10] Z. Kaplan, B. Ipekoglu, Characteristics of Mortars of Mosaics from A Roman Villa in Antandros Ancient City, Turkey. 2013.

[11] M. I. Almeida, Características geotécnicas dos solos de Lisboa. Dissertação de Doutoramento na Especialidade de Geotecnia, Universidade de Lisboa, 1991, pp.391. [in Portuguese]

[12] J. L. Zêzere, The North of Lisbon Region - A Dynamic Landscape, Landscapes and Landforms of Portugal, World Geomorphological Landscapes, Springer, 2020, pp. 265–272. DOI: 10.1007/978-3-319-03641-0_20

[13] G. Artioli, Scientific methods and cultural heritage. An introduction to the application of materials sciences to archaeometry and conservation science, New York, US: Oxford University Press, 2010, pp.47-55.

[14] A. Moropoulou, A. Bakolas, K. Bisbikou, Investigation of the Technology of Historic Mortars, Journal of Cultural Heritage, vol.1, 2000, pp. 45-48. DOI: 10.1016/S1296-2074(99)00118-1

[15] A. Bakolas, G. Biscontin, A. Moropoulou, E. Zendri, Characterization of Structural Byzantine Mortars by Thermogravimetric Analysis, Thermochimica Acta, vol.321/1-2, 1998, pp. 151-160. DOI: 10.1016/S0040-6031(98)00454-7

[16] J. Elsen, K. Van Balen, G. Mertens, Hydraulicity in Historic Lime Mortars: A Review, RILEM Book series 7 (September), 2013, pp. 125–39. DOI: 10.1007/978-94-007-4635-0_10